

WL-TR-96-2039



**STARTUP OF THE LIQUID-METAL HEAT PIPE
IN AERODYNAMIC HEATING ENVIRONMENTS**

FEBRUARY 1996

FINAL REPORT FOR 07/01/95--01/31/96

Approved for public release; distribution unlimited

**WON S. CHANG
AERO PROPULSION AND POWER DIRECTORATE
WRIGHT LABORATORY
AIR FORCE MATERIEL COMMAND
WRIGHT-PATTERSON AIR FORCE BASE, OH 45433-7251**

19960424 091

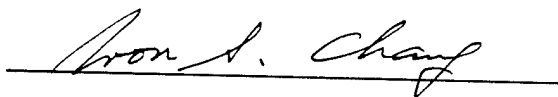
DTIC QUALITY INSPECTED 1

NOTICE

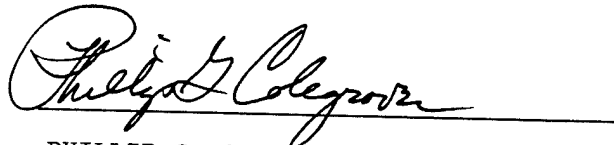
When Government drawings, specifications, or other data are used for any purpose other than in connection with a definitely Government-related procurement, the United States Government incurs no responsibility or any obligation whatsoever. The fact that the government may have formulated or in any way supplied the said drawings, specifications, or other data, is not to be regarded by implication, or otherwise in any manner construed, as licensing the holder, or any other person or corporation; or as conveying any rights or permission to manufacture, use, or sell any patented invention that may in any way be related thereto.

This report is releasable to the National Technical Information Service (NTIS). At NTIS, it will be available to the general public, including foreign nations.

The technical report has been reviewed and is approved for publication.



WON S. CHANG
Project Engineer
Power Technology Branch



PHILLIP G. COLEGROVE
Power Technology Branch



MICHAEL D. BRAYDICH, LT COL, USAF
Chief, Aerospace Power Division
Aero Propulsion and Power Directorate

If your address has changed, if you wish to be removed from our mailing list, or if the addressee is no longer employed by your organization please notify WL/POOS, Wright-Patterson AFB OH 45433-7251 to help maintain a current mailing list.

Copies of this report should not be returned unless return is required by Security Consideration, contractual obligations, or notice on a specific document.

REPORT DOCUMENTATION PAGE			Form Approved OMB No. 0704-0188	
<small>Public reporting burden for this collection of information is estimated to average 1 hour per response, including the time for reviewing instructions, searching existing data sources, gathering and maintaining the data needed, and completing and reviewing the collection of information. Send comments regarding this burden estimate or any other aspect of this collection of information, including suggestions for reducing this burden, to Washington Headquarters Services, Directorate for Information Operations and Reports, 1215 Jefferson Davis Highway, Suite 1204, Arlington, VA 22202-4302, and to the Office of Management and Budget, Paperwork Reduction Project (0704-0188), Washington, DC 20503</small>				
1. AGENCY USE ONLY (Leave blank)	2. REPORT DATE February 1996	3. REPORT TYPE AND DATES COVERED Final 7/1/95-1/31/96		
4. TITLE AND SUBTITLE Startup of the Liquid-Metal Heat Pipe in Aerodynamic Heating Environments		5. FUNDING NUMBERS PE 62 PR 3145 TA 20 WU 49		
6. AUTHOR(S) Won S. Chang				
7. PERFORMING ORGANIZATION NAME(S) AND ADDRESS(ES) Aero Propulsion and Power Directorate Wright Laboratory Air Force Materiel Command Wright-Patterson AFB, OH 45433-7251		8. PERFORMING ORGANIZATION REPORT NUMBER WL-TR-96-2039		
9. SPONSORING / MONITORING AGENCY NAME(S) AND ADDRESS(ES) Structures Directorate Research, Development and Engineering Center U.S. Army Missile Command Redstone Arsenal, AL 35898-5247		10. SPONSORING / MONITORING AGENCY REPORT NUMBER WL-TR-96-2039		
11. SUPPLEMENTARY NOTES				
12a. DISTRIBUTION AVAILABILITY STATEMENT Approved for Public Release; Distribution is Unlimited			12b. DISTRIBUTION CODE	
13. ABSTRACT (Maximum 200 words) As part of a US Army missile development program, liquid-metal heat pipes have been investigated to remove the high heat flux associated with the missile fins being located in hot exhaust gas paths. Using steady-state and transient analyses, a solution method has been developed to identify the required length of the condenser for a design operation when the heat pipe is coupled with aerodynamic heating and cooling environments. A simple transient analysis using the lumped heat-capacity method predicts the response of operating temperatures and the propagation of the continuum front when the liquid-metal heat pipe is started from the frozen state.				
14. SUBJECT TERMS Missile Fin Cooling, Liquid-Metal Heat Pipe			15. NUMBER OF PAGES 50	
			16. PRICE CODE	
17. SECURITY CLASSIFICATION OF REPORT Unclassified	18. SECURITY CLASSIFICATION OF THIS PAGE Unclassified	19. SECURITY CLASSIFICATION OF ABSTRACT Unclassified	20. LIMITATION OF ABSTRACT SAR	

TABLE OF CONTENTS

LIST OF FIGURES	iv
LIST OF TABLES	v
NOMENCLATURE	vi
ACKNOWLEDGEMENTS	x
INTRODUCTION	1
FORCED CONVECTION HEAT TRANSFER IN HIGH SPEED FLOW	4
STEADY-STATE ANALYSIS	8
TRANSIENT ANALYSIS	16
CONCLUSIONS AND RECOMMENDATIONS	24
APPENDIX: LISTING OF THE COMPUTER PROGRAM	29
REFERENCES:	40

LIST OF FIGURES

Figure	Page
1. Schematic of exhaust jets and fins of the missile.	2
2. Cross-section of the heat pipe fin.	3
3. Flow conditions of free streams.	5
4. Schematic of the heat pipe with temperature locations.	10
5. Propagation of the continuum front.	20
6. Temperature response of the fore heat pipe.	22
7. Continuum front propagation of the fore heat pipe.	23
8. Temperature response of the aft heat pipe.	25
9. Continuum front propagation of the aft heat pipe.	26

LIST OF TABLES

Table	Page
I. Physical Properties of Sodium	15
II. Fore Heat Pipe Details	15
III. Calculated Results for the Fore Heat Pipe	16
IV. Input Data for Startup Prediction for the Aft Heat Pipe	21

NOMENCLATURE

A	surface area
A_p	cross-sectional area of pipe wall
A_v	cross-sectional area of vapor core
A_w	cross-sectional area of wick structure
c_p	specific heat at constant pressure
C	effective volumetric heat capacity per unit spanwise length
C_f	effective volumetric heat capacity of free molecular flow region
d	diameter of screen wire
D	diameter of heat pipe
f_v	Fanning friction factor for vapor flow
F_l	friction coefficient for liquid flow
F_v	friction coefficient for vapor flow
g	gravitational acceleration
h	average heat transfer coefficient
h_c	average heat transfer coefficient at condenser
h_e	average heat transfer coefficient at evaporator
h_{fg}	latent heat of vaporization
h_{sl}	latent heat of fusion
h_x	local heat transfer coefficient at x
h_θ	local heat transfer coefficient at θ
k	thermal conductivity of fluid
k_e	effective thermal conductivity of liquid-saturated wick
$k_{e,c}$	effective thermal conductivity of condenser wick
$k_{e,e}$	effective thermal conductivity of evaporator wick
k_l	thermal conductivity of liquid
k_p	thermal conductivity of pipe material
k_w	thermal conductivity of wick material

K	permeability of wick structure
Kn	Knudsen number
l	characteristic length for Knudsen number
L	length from stagnation point to trailing edge along the surface
M_g	Mach number of exhaust gas
M_∞	Mach number of free stream
$M_{\alpha,c}$	stream Mach number at condenser
$M_{\alpha,e}$	stream Mach number at evaporator
N	mesh number of screen
Nu_x	local Nusselt number
Nu_L	average Nusselt number
Pr	Prandtl number
q_r	radial heat flux
Q	heat transfer rate
Q_c	heat removal rate from condenser
Q_{cap}	capillary limit on heat transport capability
Q_e	heat load to evaporator
Q_{ent}	entrainment limit on heat transport capability
Q_f	heat transferred from continuum region to free molecular region
Q_s	sonic limit of heat transport capability
r	recovery factor
r_c	recovery factor at condenser
r_e	recovery factor at evaporator
$r_{h,s}$	hydraulic radius of wick at liquid-vapor interface
r_i	inside radius of heat pipe
r_o	outside radius of heat pipe
r_v	radius of vapor core
R	gas constant
Re_D	Reynolds number for fluid flow over cylinder

Re_L	Reynolds number for fluid flow over plate at $x = L$
Re_v	Reynolds number for vapor flow
Re_x	Reynolds number for fluid flow over plate at x
T_{fc}	temperature in free molecular region
T_g	temperature of exhaust gas
T_m	melting temperature
T_o	stagnation temperature
T_p	pipe wall temperature or lumped temperature
$T_{p,c}$	temperature of condenser pipe wall
$T_{p,e}$	temperature of evaporator pipe wall
$T_{pw,c}$	pipe-wick interface temperature of condenser
$T_{pw,e}$	pipe-wick interface temperature of evaporator
T_r	recovery temperature
T_t	transition temperature
T_v	vapor temperature
T_∞	free-stream temperature
$T_{\infty,c}$	free-stream temperature at condenser
$T_{\infty,e}$	free-stream temperature at evaporator
T^*	reference temperature
u	free-stream velocity
v	mean molecular velocity
x	axial location on plate
x_o	location beyond which the flat plate correlation applies
z	axial location on heat pipe
z_c	condenser length
z_e	evaporator length
z_{eff}	effective heat pipe length
γ	ratio of specific heats
Δt	time increment

ϵ	porosity of wick structure
θ	angle
λ	mean free path
μ_l	liquid viscosity
μ_v	vapor viscosity
ρ_l	liquid density
ρ_v	vapor density
σ	surface tension

Subscripts

c	condenser
e	evaporator
l	liquid
s	solid
v	vapor
w	wick

Superscripts

n	time at $n\Delta t$
$n+1$	time at $(n+1)\Delta t$

ACKNOWLEDGMENTS

Foremost, I would like to thank Jeffrey R. Brown for his help with the computer program. Thanks are also due to John E. Leland for his careful reading of the manuscript and his valuable suggestions. In addition, I wish to express my gratitude to Bill Nourse at US Army Missile Command for the financial support.

For an expert typing of the manuscript special thanks are given to Janice M. Schlemmer. My thanks are extended to Mike Bruggeman for preparing excellent drawings.

INTRODUCTION

The feasibility of employing heat pipes to cool the hot sections of the Army's ground-to-ground missile fins has been studied. A portion of each fin is exposed directly to the hot gas from the exhaust jet. The rest of the fin is in an air stream. Heat pipes integrated into the fin structure are proposed for transferring heat from the hot section to the cool section of the fin to prevent damage to the fin during the missile's ten-minute flight. A part of the missile, showing the location of fins with respect to the exhaust jets, is depicted in Fig. 1. The fin considered in this study is a thin airfoil and its planform is rectangular. The fin surface is symmetrical with respect to the chord line; that is, the mean chamber line is coincident with the chord line. The angle of attack is zero so that the free-stream flow is parallel to the chord line.

The proposed fin cooling concept consists of two liquid-metal heat pipes separated by a planar rib as shown in Fig. 2. Liquid metal has been considered as the working fluid for both heat pipes because high operating temperatures are anticipated. However, the use of liquid metal creates a startup problem since the working fluid is initially in a solid state at ambient temperature. These heat pipes thus need to be designed so that they start successfully from the frozen state. For this purpose, a simple model based on the lumped heat-capacity method has been developed for predicting the startup and transient characteristics. The surface of the fore heat pipe in the leading edge region has much higher heat flux than the heat pipe located in the rear. Therefore, in addition to the transient analysis, a steady-state analysis has been performed for the fore heat pipe to determine whether the heat pipe will operate as designed.

In order to determine the heat load to the evaporator and the heat removal rate from the condenser for the fore and aft heat pipes, it is necessary to evaluate the heat transfer coefficients between the surface of the airfoil fin and the heat source and sink. A fairly good approximation may be made by use of the heat transfer correlations for smooth cylinders and flat plates for the fore and aft heat pipes, respectively. The fore heat pipe may be geometrically transformed to a circular cylinder of equivalent diameter. The aft heat pipe following the equivalent cylinder can be analyzed using the flat plate correlations.

There are two free-stream flows: exhaust gas stream and air stream. The Mach number and

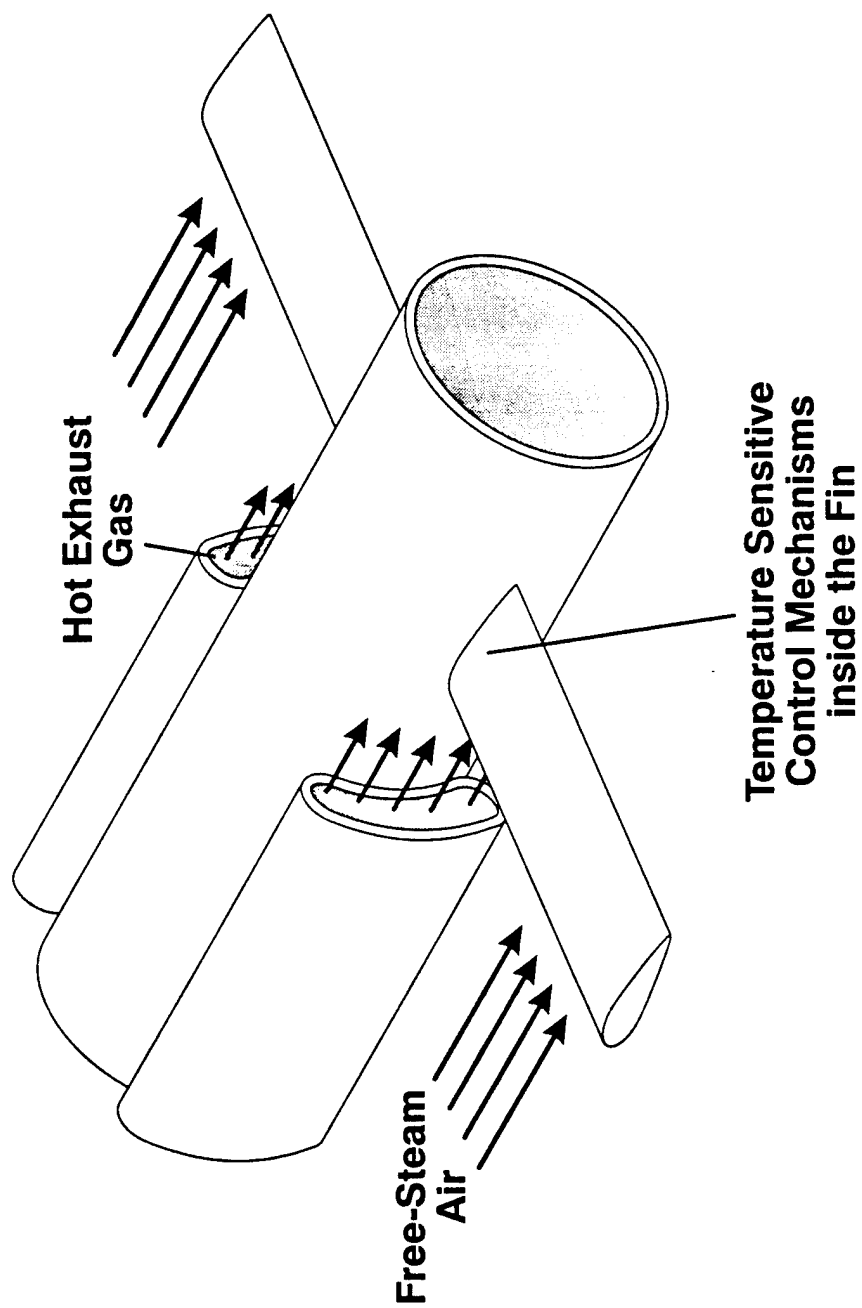


Fig. 1 Schematic of exhaust jets and fins of the missile.

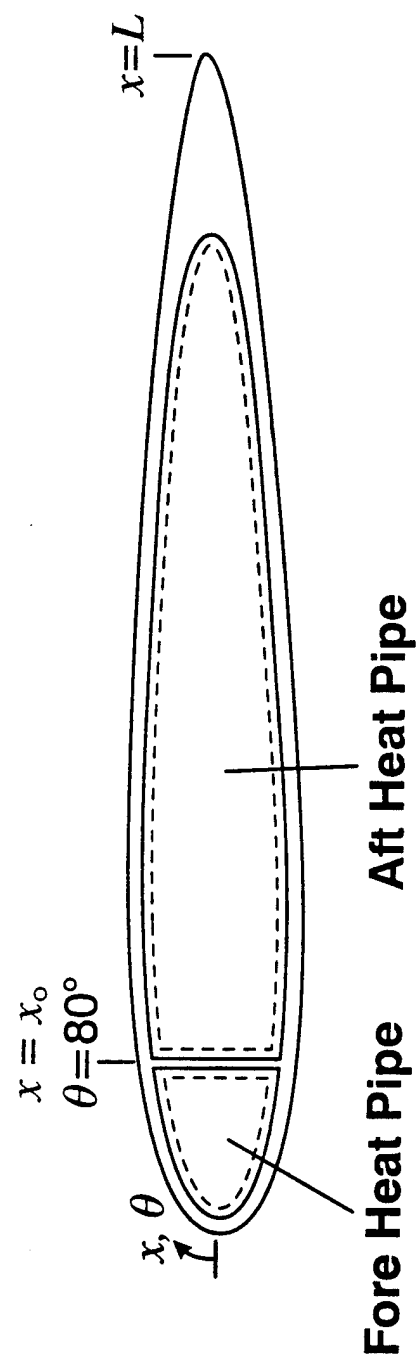


Fig. 2 Cross-section of the heat pipe fin.

static temperature of each stream are indicated in Fig. 3. Since the exhaust gas flow is supersonic, a curved shock wave exists in front of the leading edge. To simplify the analysis, a normal shock is assumed instead of the curved shock. After the normal shock, the Mach number and static temperature of the gas become $M_e=0.8892$ and $T_{\infty,e}=1084\text{K}$ as can be calculated from the normal shock tables (John, 1984).

FORCED CONVECTION HEAT TRANSFER IN HIGH-SPEED FLOW

The startup and steady-state characteristics of liquid-metal heat pipes depend on the heat source and heat sink conditions. For the conditions of interest, radiation heat transfer has been considered and found negligible compared to the aerodynamic heating. Therefore, only aerodynamic heating and cooling heat transfer rates are considered here. Considering heat transfer on the surface of heat pipes moving at high velocities in the hot exhaust gas and air stream, the effects of the fluid compressibility and viscous dissipation must be taken into account.

The heat transfer rate Q on the surface in high-speed flow can be calculated with the same relations used for low-speed flow if the average heat transfer coefficient h is defined as

$$Q = hA(T_p - T_r) \quad (1)$$

where A is the surface area, T_p is the surface temperature, and T_r is the recovery temperature. The recovery temperature is expressed by a dimensionless parameter, r , called the temperature recovery factor and defined as

$$r = \frac{T_r - T_\infty}{\left(\frac{u^2}{2c_p} \right)} \quad (2)$$

or

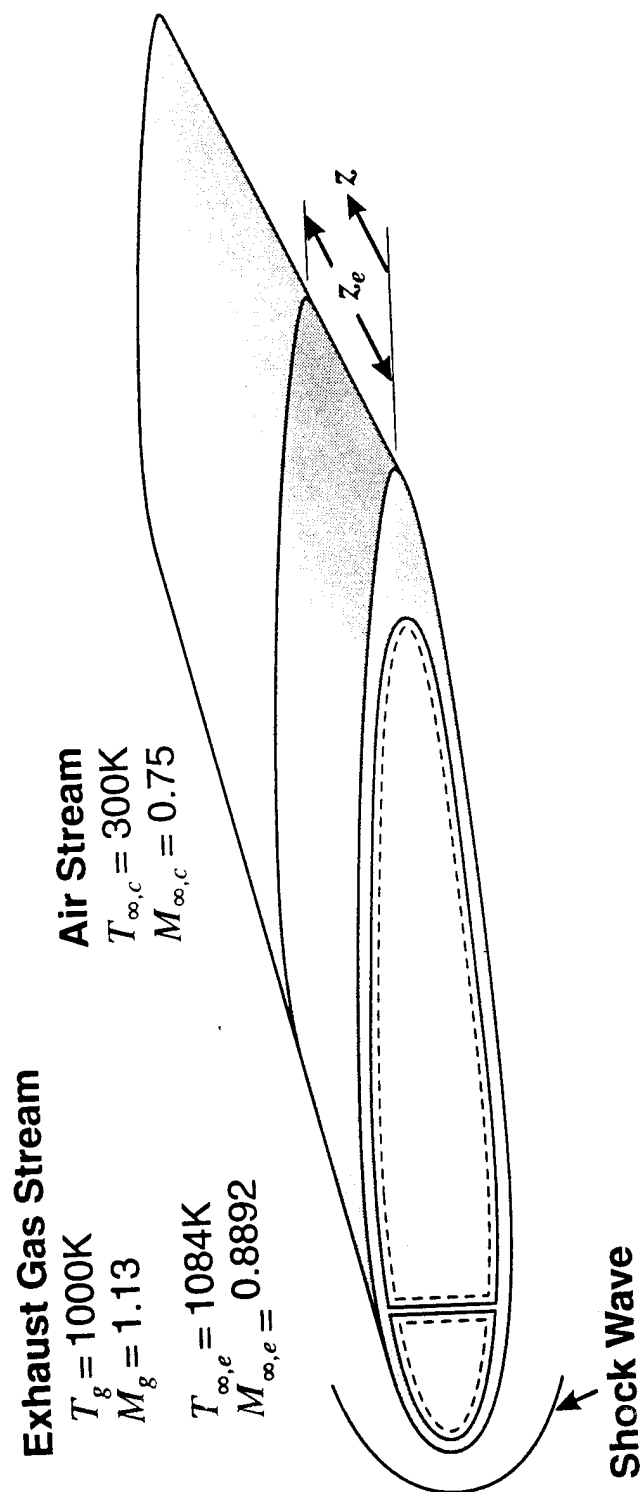


Fig. 3 Flow conditions of free streams.

$$r = \frac{T_r - T_\infty}{T_o - T_\infty} \quad (3)$$

where T_∞ is the free-stream temperature, u is the free-stream velocity, c_p is the specific heat at constant pressure of the fluid, and T_o is the stagnation temperature.

Stagnation temperature for a perfect gas with constant specific heats is found from

$$T_o = T_\infty \left(1 + \frac{u^2}{2c_p T_\infty} \right) \quad (4)$$

Expressing this equation in terms of the Mach number gives

$$T_o = T_\infty \left(1 + \frac{\gamma-1}{2} M_\infty^2 \right) \quad (5)$$

where γ is the ratio of specific heats of the fluid. Experiments with flat plates have shown that the recovery factor r can be approximately expressed in terms of the Prandtl number Pr . For laminar flow,

$$r = Pr^{1/2} \quad (6)$$

whereas for turbulent flow,

$$r = Pr^{1/3} \quad (7)$$

In order to account for fluid property dependence on temperature, Eckert (1960) has recommended that the properties be evaluated at a reference temperature T^* given by

$$T^* = T_\infty + 0.5(T_p - T_\infty) + 0.22(T_r - T_\infty) \quad (8)$$

The last term in Eq. (8) can also be expressed by the Mach number as

$$T^* = T_\infty + 0.5(T_p - T_\infty) + 0.11(\gamma-1)rM_\infty^2 T_\infty \quad (9)$$

The leading edge contour may be approximated by a cylindrical shape which has the same circumference. Over the forward portion of the cylinder ($0^\circ < \theta < 80^\circ$) where the angle θ is measured from the stagnation point, the empirical equation for the local heat transfer coefficient h_θ at θ is given as

$$\frac{h_\theta D}{k} = 1.14 Re_D^{1/2} Pr^{2/5} \left[1 - \left(\frac{\theta}{90} \right)^3 \right] \quad (10)$$

where k is the thermal conductivity of fluid and Re_D is the Reynolds number based on the diameter D . That is,

$$Re_D = \frac{\rho u D}{\mu} \quad (11)$$

where ρ and μ are the density and viscosity of the fluid. Equation (10) was originally presented by Martinelli et al. (1943) for the range of θ from 0° to 90° . However, Kreith and Bohn (1986) suggested to use this equation from 0° to 80° , as has been done in the present work. Integrating Eq. (10) along the arc length from 0 to $2\pi D/9$ with respect to $D\theta/2$, the average heat transfer coefficient h becomes

$$\frac{h D}{k} = 0.94 Re_D^{1/2} Pr^{2/5} \quad (12)$$

The heat transfer rate on the surface following the leading edge region may be evaluated by treating the surface as two flat plates. The flow is assumed turbulent over the entire surface because of the expected free-stream turbulence. The local heat transfer coefficient h_x for the turbulent boundary layer on a flat plate is given by (Chapman, 1984)

$$Nu_x = \frac{h_x x}{k} = 0.0296 Re_x^{4/5} Pr^{1/3} \quad (13)$$

when the Reynolds number ranges from 5×10^5 to 10^7 which encompasses the range of flow conditions considered in this study. Here, the characteristic length x is the distance starting from the stagnation

point. Integrating Eq. (13) along the plate length L from x_o to obtain the average heat transfer coefficient h gives

$$Nu_L = \frac{hL}{k} = 0.037 Re_L^{4/5} Pr^{1/3} \frac{1 - \left(\frac{x_o}{L}\right)^{4/5}}{1 - \frac{x_o}{L}} \quad (14)$$

STEADY-STATE ANALYSIS

The leading edge region of the missile fin is subjected to a severe aerodynamic heating environment. Therefore, the fore heat pipe must be able to handle the high heat flux by distributing the heat around the whole circumference of the wick structure. For this purpose, it is desirable to use a wick structure possessing circumferentially interconnecting pores. As an example, the present study analyzes a screen wick saturated with liquid sodium for characterizing the heat pipe performance at steady state. The operating condition of the fore heat pipe must be below the operating limits on its heat transport capability.

Since the operating temperature and the condenser length of the heat pipe required to remove the heat load are not known a priori, iterative calculations are necessitated. First, the surface temperature of the evaporator $T_{p,e}$ is assumed. From the aerodynamic heating correlations, the heat load to the evaporator can then be found. Because at steady state the total heat input to the evaporator must be rejected through the condenser surface to the heat sink, the required length of the condenser can be determined. Once the operating temperature of the heat pipe is calculated, all the operating limits on the heat transport capability are evaluated at that operating temperature. If the operating condition exceeds any operating limit, a new value of the surface temperature of the evaporator is assumed and the above calculating procedure must be repeated until successful operation is obtained.

The heat transfer rate to the cylindrical surface of the evaporator, subtended by the angle $\theta = 8\pi/9$, can be obtained from

$$Q_e = h_e \left(\frac{4}{9} \pi D z_e \right) (T_{p,e} - T_{r,e}) \quad (15)$$

where z_e is the given evaporator length and the subscript e denotes the evaporator. The average heat transfer coefficient for the evaporator surface, h_e , in Eq. (15) can be calculated from Eq. (12). Assuming that the heat applied to a portion of the circumference of the heat pipe may be distributed equally through the entire heat pipe periphery at steady state, the radial heat flux can be expressed as

$$q_r = \frac{Q_e}{\pi D z_e} \quad (16)$$

This assumption can be made because liquid metal has a thermal conductivity large enough to spread the partially applied heat around the circumference.

It is important to determine the operating temperature of the heat pipe. The temperature difference between the vapor and the liquid at the liquid-vapor interface is generally small and can be neglected. Furthermore, the temperature of the vapor core may be assumed to be uniform because of the small thermal resistance for vapor flow. Accordingly, the primary temperature drops in the heat pipe occur through the pipe wall and the liquid-saturated wick.

Figure 4 shows the locations where temperatures have been evaluated and the dimensions of the heat pipe. Applying the Fourier law of heat conduction, the individual temperature drops can be written as follows :

$$T_{p,e} - T_{pw,e} = \frac{\ln \frac{r_o}{r_i}}{2 \pi z_e k_p} Q_e \quad (17)$$

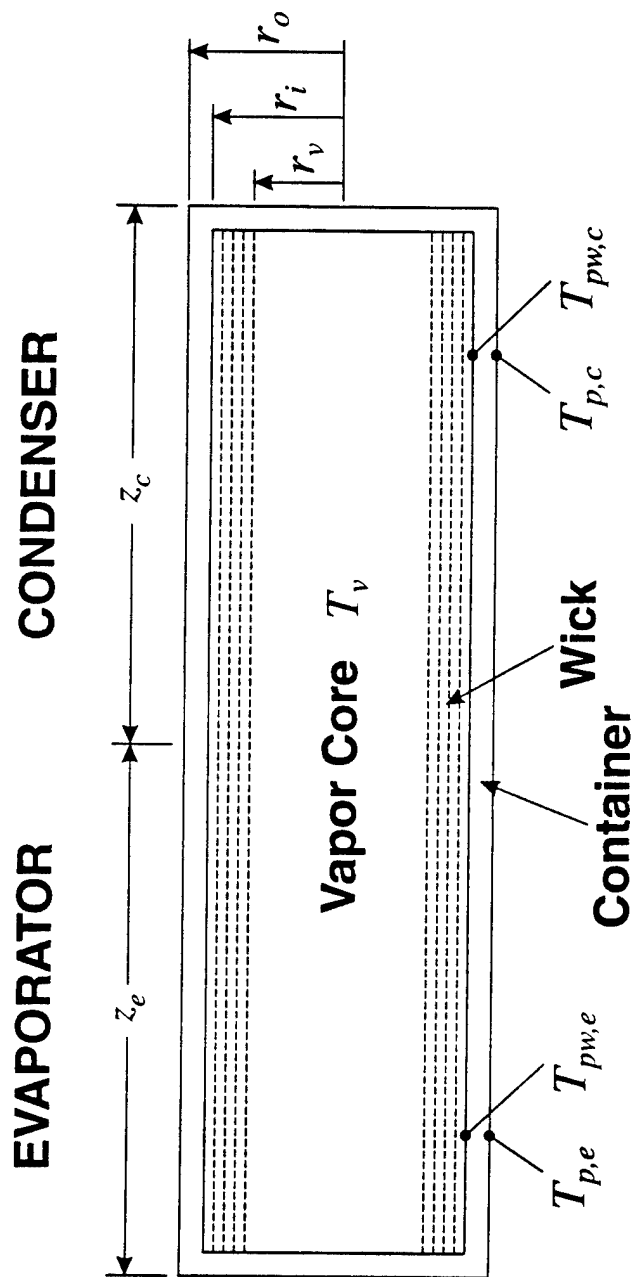


Fig. 4 Schematic of the heat pipe with temperature locations.

$$T_{pw,e} - T_v = \frac{\ln \frac{r_i}{r_v}}{2\pi z_e k_{e,e}} Q_e \quad (18)$$

$$T_v - T_{pw,c} = \frac{\ln \frac{r_i}{r_v}}{2\pi z_c k_{e,c}} Q_e \quad (19)$$

$$T_{pw,c} - T_{p,c} = \frac{\ln \frac{r_o}{r_i}}{2\pi z_c k_p} Q_e \quad (20)$$

In the above equations, the subscripts e and c indicate the evaporator and the condenser and k_p is the thermal conductivity of pipe material. The temperatures T_p , T_{pw} , and T_v are the temperature of the pipe wall surface, the temperature at the pipe-wick interface, and the vapor temperature, respectively. The radii r_o , r_i , and r_v are for the outside and inside of the pipe and the vapor core. The effective thermal conductivity k_e for the liquid-saturated screen wick in Eqs. (18) and (19) can be found from

$$k_e = \frac{k_l[(k_l + k_w) - (1-\epsilon)(k_l - k_w)]}{(k_l + k_w) + (1-\epsilon)(k_l - k_w)} \quad (21)$$

where ϵ is the porosity of the wick structure, k_l is the thermal conductivity of the liquid, and k_w is the thermal conductivity of the wick material.

Notice that the required length of the condenser z_c in Eqs. (19) and (20) to remove the applied heat load is unknown. This length must be determined such that the operating temperature of the heat pipe is within a safe range to avoid damage to the heat pipe.

During steady-state operation, all the heat applied to the evaporator will be rejected through the surface of the condenser. The equation used for the aerodynamic heating on the evaporator surface can also be employed for the aerodynamic cooling on the condenser surface by changing the sign. The heat removal rate from the condenser can then be found from

$$Q_c = h_c \left(\frac{4}{9} \pi D z_c \right) (T_{r,c} - T_{p,c}) \quad (22)$$

In Eq. (22), h_c and $T_{r,c}$ require the reference temperature T^* which in turn requires knowledge of $T_{p,c}$. In order to evaluate $T_{p,c}$, the unknown z_c in Eqs. (19) and (20) must be assumed so that Eq. (22) is satisfied. If the heat output from Eq. (22) is not equal to the heat input from Eq. (15), then a new value of z_c has to be assumed and the above calculation procedure needs to be repeated until a satisfactory check is made.

Using the described technique, the operating condition of the heat pipe can be analyzed. In order to confirm whether the heat pipe operates satisfactorily under this condition, the maximum heat transport capability of the heat pipe at the operating temperature must be evaluated to see if it exceeds the design condition. There are several operating limits on the heat pipe: sonic, entrainment, capillary, and boiling limits. Among these operating limits, the lowest one at a given operating temperature provides the maximum possible value of heat transfer rate at that temperature. The boiling limit is usually not a problem with liquid-metal heat pipes because of the high thermal conductivity of the fluid and the high superheat needed to initiate boiling. The most common heat transfer limit is the capillary limit. The capillary limit presented here is for the most extreme condition; that is, the heat pipe is in a vertical position with the evaporator above the condenser. The sonic, entrainment, and capillary limits can be calculated from the expressions below (Chi, 1976).

Sonic limit:

When the heat pipe is operating at low vapor densities, the vapor velocity may reach the speed of sound. For this situation the heat transport capability of the heat pipe is restricted to a maximum value by the existence of shocked flow at the evaporator exit. This restriction on the heat transport capability is known as the sonic limit.

Assuming negligible frictional effects, the vapor flow analysis gives the sonic limit Q_s as

$$Q_s = A_v \rho_v h_{fg} \left[\frac{\gamma R T_v}{2(\gamma+1)} \right]^{1/2} \quad (23)$$

where A_v is the cross-sectional area of the vapor core, ρ_v is the vapor density, h_{fg} is the latent heat of vaporization, and R is a gas constant.

Entrainment limit:

During the heat pipe operation the liquid and the vapor flow in opposite directions. If the vapor velocity is sufficiently high, a shear force exerted by the vapor at the liquid-vapor interface may entrain droplets of liquid and carry them to the condenser end. When this happens, the wick in the evaporator is depleted of liquid needed for continuous evaporation. This limits the maximum axial heat transport capability and is called the entrainment limit.

The entrainment limit Q_{ent} is determined from

$$Q_{ent} = A_v h_{fg} \left(\frac{\sigma \rho_v}{2 r_{h,s}} \right)^{1/2} \quad (24)$$

where σ is the surface tension of liquid, and $r_{h,s}$ is the hydraulic radius of the wick surface pores. The hydraulic radius of the screen wick can be found from

$$r_{h,s} = \frac{1}{2} \left(\frac{1}{N} - d \right) \quad (25)$$

where N and d are the mesh number and the wire diameter of the screen.

Capillary limit:

The maximum capillary pressure must be greater than the total pressure drop associated with the liquid and vapor flows in the heat pipe for a normal operation. Otherwise, the wick will dry out in the evaporator due to insufficient capillary pumping capability to return the liquid to the evaporator from the condenser. This operating limit is referred to as the capillary limit.

When the liquid and vapor flows are laminar and incompressible with uniform heat fluxes applied to the evaporator and condenser sections, the capillary limit Q_{cap} can be found from

$$Q_{cap} = \frac{\frac{2\sigma}{r_c} - \rho_l g(z_e + z_c)}{z_{eff}(F_l + F_v)} \quad (26)$$

where r_c is the effective capillary radius of the wick structure, ρ_l is the liquid density, and g is the gravitational acceleration. The effective heat pipe length z_{eff} is defined as

$$z_{eff} = \frac{1}{2} (z_e + z_c) \quad (27)$$

The friction coefficients for the liquid and vapor flows, F_l and F_v , are evaluated from

$$F_l = \frac{\mu_l}{KA_w \rho_l h_{fg}} \quad (28)$$

and

$$F_v = \frac{(f_v Re_v) \mu_v}{2A_w r_v^2 \rho_v h_{fg}} \quad (29)$$

In the above equations, μ_l and μ_v are the liquid and vapor viscosities, K is the permeability of the wick structure, and f_v and Re_v are the Fanning friction factor and the Reynolds number of the vapor flow.

Because of the expected high operating temperature, a sodium heat pipe has been considered for the fore heat pipe. Various physical properties of sodium are summarized in Table I. The container material is type 304 stainless steel and the wick is four layers of 200 mesh screen of type 304 stainless steel. A summary of the sodium heat pipe is given in Table II. With the given free-stream conditions shown in Fig. 3, a heat transfer rate of $Q_e=204\text{W}$ has been determined. The average radial heat flux is $q_r=13\text{ W/cm}^2$. The calculated results are listed with the operating limits in Table III. As can be noticed, all the limits are much higher than the required heat transfer rate. Therefore, it may be concluded that the sodium heat pipe with the total length of 0.078 m operates successfully under given heat source and sink conditions.

Table I. Physical Properties of Sodium

Molecular Weight	22.991
Melting Point	371.0K
Boiling Point at 1 atm	1151.2K
Critical Temperature	2500K
Critical Pressure	370 bar
Critical Density	180 kg/m ³
Latent Heat of Fusion	113.044 kJ/kg
Latent Heat of Vaporization at 1151.2K	3927.1 kJ/kg
Liquid Thermal Conductivity at 900K	61.4 W/m-K
Vapor Thermal Conductivity at 900K	4.06 X 10 ⁻² W/m-K
Liquid Viscosity at 900K	2.02 X 10 ⁻⁴ N-s/m ²
Vapor Viscosity at 900K	2.06 X 10 ⁻⁵ N-s/m ²
Surface Tension at 900K	0.142 N/m

Table II. Fore Heat Pipe Details

Working Fluid	Sodium (Na)
Container Material	Type 304 Stainless Steel
Total Heat Pipe Length	0.078 m
Evaporator Length	0.05 m
Condenser Length	0.028 m
Container Outside Diameter	0.01 m
Container Inside Diameter	0.007 m
Wick Material	Type 304 Stainless Steel
Wick Structure	Four Layers of 200 Mesh Screen

Table III. Calculated Results for the Fore Heat Pipe

$Q_e = 204\text{W}$	$q_r = 13 \text{ W/cm}^2$
$r_e = 0.8526$	$r_c = 0.8289$
$T_{r,e} = 1211.7\text{K}$	$T_{r,c} = 326.6\text{K}$
$T_e^* = 1055.1\text{K}$	$T_c^* = 625.5\text{K}$
$T_{p,e} = 970\text{K}$	$T_{p,c} = 939.3\text{K}$
$T_{pw,e} = 960.7\text{K}$	$T_{pw,c} = 956\text{K}$
$T_v = 959\text{K}$	
Sonic Limit, $Q_s = 1764.9 \text{ W}$	
Entrainment Limit, $Q_{ent} = 1121.3\text{W}$	
Capillary Limit, $Q_{cap} = 441 \text{ W}$	

It is of importance to notice that the steady-state analysis mentioned above is restricted to the situation when there is no free molecular region in the heat pipe. If the heat pipe is steadily operating with a portion of the free molecular region in the inactive condenser section, the results from the steady-state analysis will be in error. As explained in the next section, the transient model predicts the existence of the free molecular region.

TRANSIENT ANALYSIS

When the liquid-metal heat pipe is started up from ambient temperature, the working substance is in the solid state. The vapor density is so small that free molecular flow regime prevails over the entire vapor core. As heat is applied to the evaporator, the frozen working substance will be melted. As heating continues, the free molecular flow in the evaporator will become continuum flow. Evaporation can, thereafter, take place at the liquid-vapor interface resulting in the increase of the vapor temperature of the evaporator. With further heating, a continuum flow front moves toward the condenser end while the sonic limit exists at the evaporator exit. Once the front has reached the end of the condenser, continuum flow exists over the entire heat pipe length. The operating temperature will then continue to rise until steady state is reached. The solution procedure

is the same for the startup prediction of the fore heat pipe and the aft heat pipe except for the calculations of the heat transfer coefficients, h_e and h_c , and the heat input and output.

The transition from the free molecular flow regime to the continuum flow regime occurs when the Knudsen number Kn is less than 0.01.

$$Kn = \frac{\lambda}{l} < 0.01 \quad (30)$$

Here, λ is the mean free path of vapor and l is a characteristic length. From kinetic theory, the dynamic viscosity μ_v and the mean molecular velocity v are

$$\mu_v = 0.499 \rho_v v \lambda \quad (31)$$

and

$$v = \sqrt{\frac{8 R T_v}{\pi}} \quad (32)$$

From Eqs. (30) - (32), it can be noticed that continuum flow exists when the temperature of the vapor reaches the transition temperature T_t given by

$$T_t = \frac{4990 \pi}{R} \left(\frac{\mu_v}{\rho_v l} \right)^2 \quad (33)$$

Iterations are required to determine T_t because of the temperature dependence of μ_v and ρ_v . The characteristic length l in Eq. (33) is the vapor core diameter for the fore heat pipe and is assumed to be the maximum thickness of the vapor core for the aft heat pipe.

The lumped heat-capacity method has been applied to the heat pipe. For the startup from the frozen state, the evaporator temperature can be found from the energy balance on the evaporator section as

$$T_p^{n+1} = T_p^n + \frac{Q_e \Delta t}{C z_e} \quad (34)$$

when $T_p^n < T_t$. Here, the superscripts n and $n+1$ denote times $t = n\Delta t$ and $t = (n+1)\Delta t$ where Δt is a time increment. The effective volumetric heat capacity per unit spanwise length C depends on whether the lumped temperature T_p^n is greater or less than the melting temperature T_m of the working substance. When $T_p^n < T_m$,

$$C = (\rho c_p)_p A_p + (1-\epsilon)(\rho c_p)_w A_w + \epsilon(\rho c_p)_s A_w \quad (35)$$

and when $T_p^n > T_m$,

$$C = (\rho c_p)_p A_p + (1-\epsilon)(\rho c_p)_w A_w + \epsilon(\rho c_p)_l A_w \quad (36)$$

The subscripts p , w , s , and l denote the pipe wall material, wick material, and the solid and liquid state of the working substance. A_p and A_w are the cross-sectional areas of the pipe wall and the wick structure. In Eqs. (35) and (36) the heat capacity of the vapor core is not included since it is negligible.

When T_p^n is greater than the transition temperature T_t , the lumped temperature T_p^{n+1} after a time increment Δt can be evaluated depending on the location of the continuum front z^n :

$$T_p^{n+1} = T_p^n + \frac{Q_e \Delta t}{C z_e} \quad (z^n \leq z_e) \quad (37)$$

$$T_p^{n+1} = T_p^n + \frac{(Q_e - Q_c - Q_f)\Delta t}{C z^n} \quad (z_e < z^n < z_e + z_c) \quad (38)$$

$$T_p^{n+1} = T_p^n + \frac{(Q_e - Q_c)\Delta t}{C(z_e + z_c)} \quad (z^n = z_e + z_c) \quad (39)$$

Q_f in Eq. (38) is the heat transferred from the continuum region to the control volume as indicated in Fig. 5 and is given by

$$Q_f = Q_s - Q_c - \rho_l \epsilon A_w h_{sl} (z^n - z^{n-1}) - \frac{C(z^n - z_e)(T_p^{n+1} - T_p^n)}{\Delta t} \quad (40)$$

Here, h_{sl} is the latent heat of fusion of the working substance.

The sonic limit Q_s in Eq. (40) can be evaluated from Eq. (23). Because of the complex cross-sectional shape of the fin, the vapor core area A_v of the aft heat pipe for Eq. (23) has been evaluated by Simpson's rule. For the fore heat pipe, the heat transfer rates are calculated from Eqs. (15) and (22) with the heat transfer coefficient from Eq. (12). For the aft heat pipe, the heat transfer coefficient for the portion of the fin following the equivalent cylinder is calculated from the flat plate equation. Using the average heat transfer coefficient from Eq. (14), the heat transfer rate to the heated and the cooled zones of the aft heat pipe can be calculated from

$$Q_e = 2h_e(L - x_o)z_e(T_{r,e}^n - T_p^n) \quad (41)$$

and

$$Q_c = 2h_c(L - x_o)(z^n - z_e)(T_p^n - T_{r,c}^n) \quad (42)$$

The location of the continuum front can be found by applying the energy balance to the small control volume of width $(z^{n+1} - z^n)$ as shown in Fig. 5.

$$z^{n+1} = z^n + \frac{Q_f \Delta t}{CT_p^{n+1} - C_f T_{fc}} \quad (43)$$

where the effective volumetric heat capacity C_f of the free molecular flow region depends on whether the temperature of the free molecular flow region T_{fc} is greater or less than the melting temperature

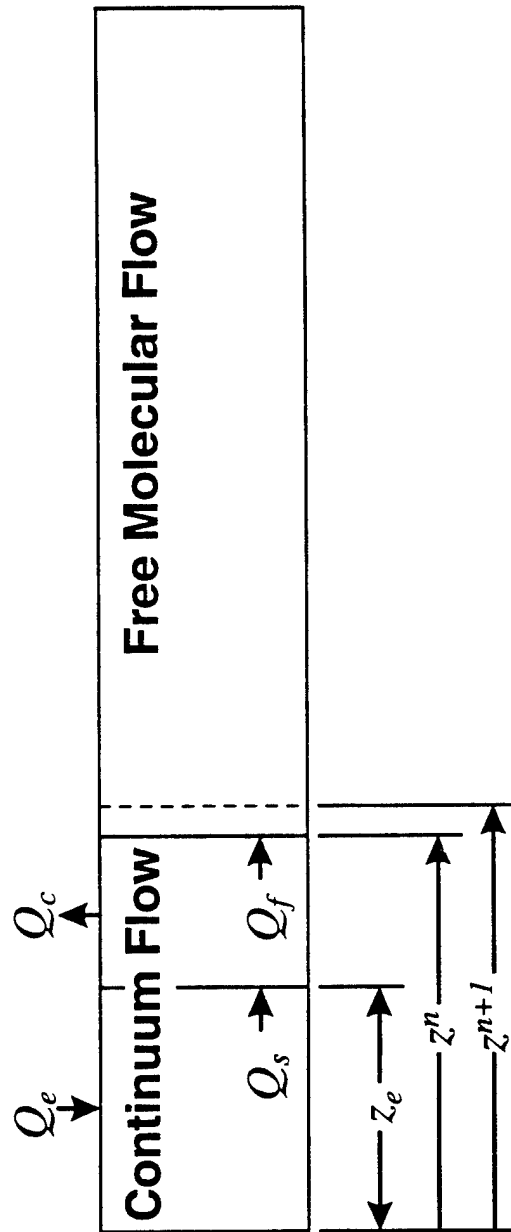


Fig. 5 Propagation of the continuum front.

T_m as in Eqs. (35) and (36).

A computer program has been developed for predicting transient startup of liquid-metal heat pipes. A listing of a Fortran version of this program is given in Appendix. The Fortran variable names assigned to the various quantities are presented in the first part of the program. The computer program consists of a main program and three subroutines. These subroutines are for the thermophysical properties of air, type 304 stainless steel, and sodium. The properties are excerpted from Brennan and Kroliczek (1979), Incropera and DeWitt (1981), and Vargaftik (1975).

The transient model has been applied to the fore and aft heat pipes to investigate the feasibility of using the liquid-metal heat pipe. Sodium is the working fluid and type 304 stainless steel is used for the container and wick structure. Descriptions of the fore and aft heat pipes are given in Tables II and IV.

The computed results for the fore heat pipe are plotted in Figs. 6 and 7. These figures show the variation of the lumped temperature and the continuum flow front as a function of time. Once the temperature exceeds the transition temperature of 725.2K, the continuum front starts to

Table IV. Input Data for Startup Prediction for the Aft Heat Pipe

Working Fluid	Sodium (Na)
Container Material	Type 304 Stainless Steel
Plate Length	0.12m
Total Available Heat Pipe Length	0.25m
Evaporator Length	0.05m
Wall Thickness	0.0015m
Wick Thickness	0.0005m
Wick Porosity	0.7
Characteristic Length	0.014m
Vapor Core Area	0.00067m ²

Fore

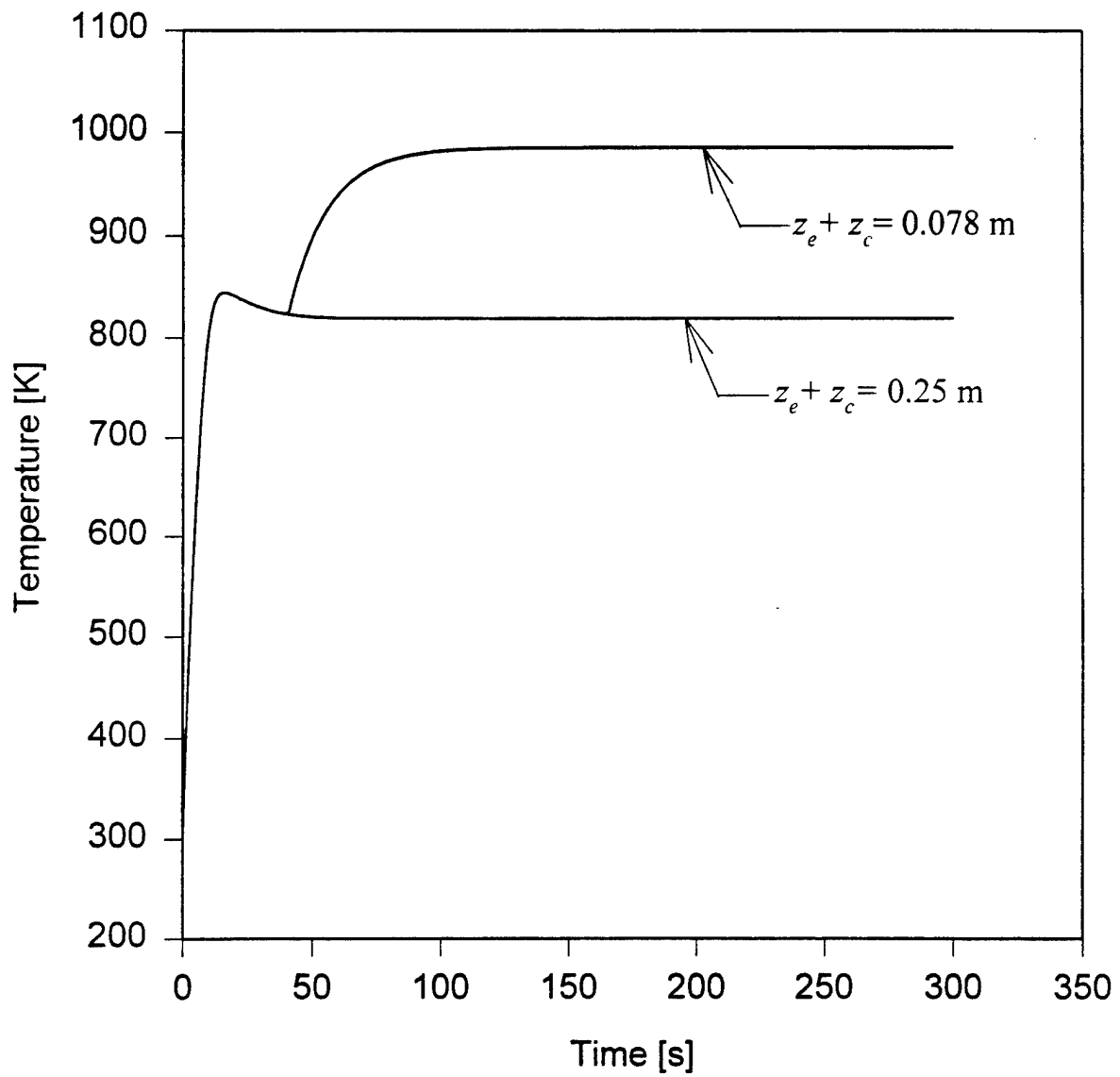


Fig. 6 Temperature response of the fore heat pipe.

Fore

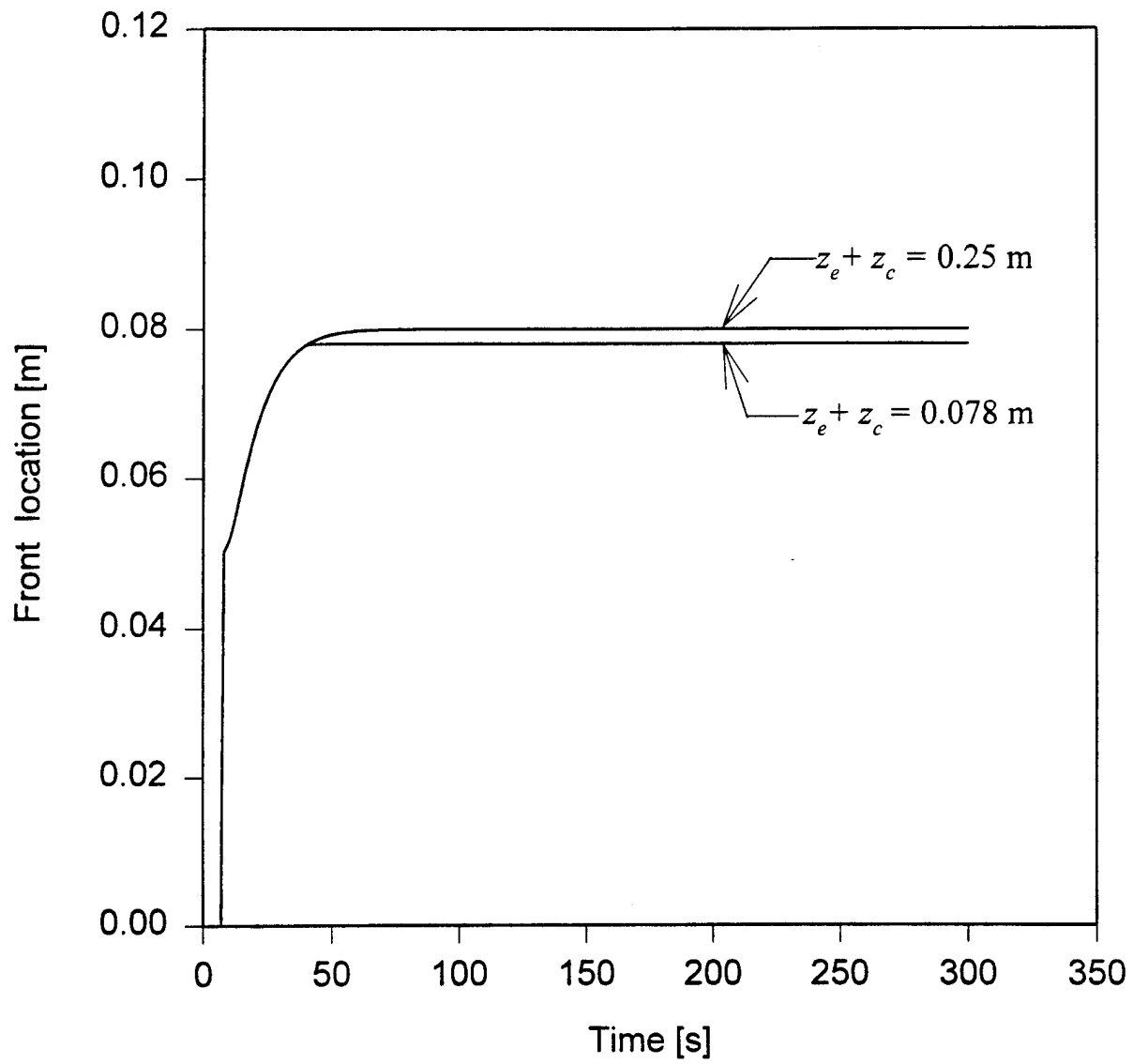


Fig. 7 Continuum front propagation of the fore heat pipe.

propagate from the evaporator exit toward the condenser end. When the total spanwise length of the fin is used as the total length of the heat pipe ($z_e + z_c = 0.25$ m), steady state is reached at 65 seconds with $T_p = 819$ K and $z = 0.08$ m. The continuum front does not move to the condenser end because the operating condition of the heat pipe is lower than the design condition. A shorter length than $z = 0.08$ m may be used for the given conditions with a much higher operating temperature; then the continuum front will reach the condenser end and a normal operation can be obtained.

Figures 6 and 7 include the computed results for $z_e + z_c = 0.078$ m which is the same length as that in the steady-state analysis. The front reaches the condenser end at 40 seconds. Thereafter, the temperature increases until steady state is reached at 120 seconds with $T_p = 985$ K. This steady operating temperature is close to $T_v = 959$ K from the steady-state analysis.

Similar calculations have been conducted for the aft heat pipe. The transition temperature is 689.1K, and the results are shown in Figs. 8 and 9. When the total length of the fin is used as the total heat pipe length, i.e., $z_e + z_c = 0.25$ m, the continuum front stops at $z = 0.1115$ m with $T_p = 810$ K after 120 seconds. When a shorter length of $z_e + z_c = 0.078$ m is used, the continuum front reaches the condenser end at 18 seconds. Since then the temperature increases until steady state is reached at 120 seconds with $T_p = 997$ K.

With a heat pipe length of 0.078 m, the operating temperature of the fore heat pipe ($T_p = 985$ K) is slightly lower than that of the aft heat pipe ($T_p = 997$ K). Even though very high heat flux is anticipated at the fore heat pipe, its operating temperature is lower due to the distributed heat input around the circumference of the wick structure.

CONCLUSIONS AND RECOMMENDATIONS

The use of heat pipes to cool the hot region of a missile fin has been studied. A steady-state analysis has been performed for the heat pipe in order to determine whether the operating condition satisfies the limitations on the heat transport capability when the heat pipe is normally operating without any free molecular region. In addition, startup characteristics of the heat pipe from the frozen state have been analyzed by a lumped heat-capacity method. This transient model provides the necessary length of the heat pipe and predicts the temperature and continuum front location until

Aft

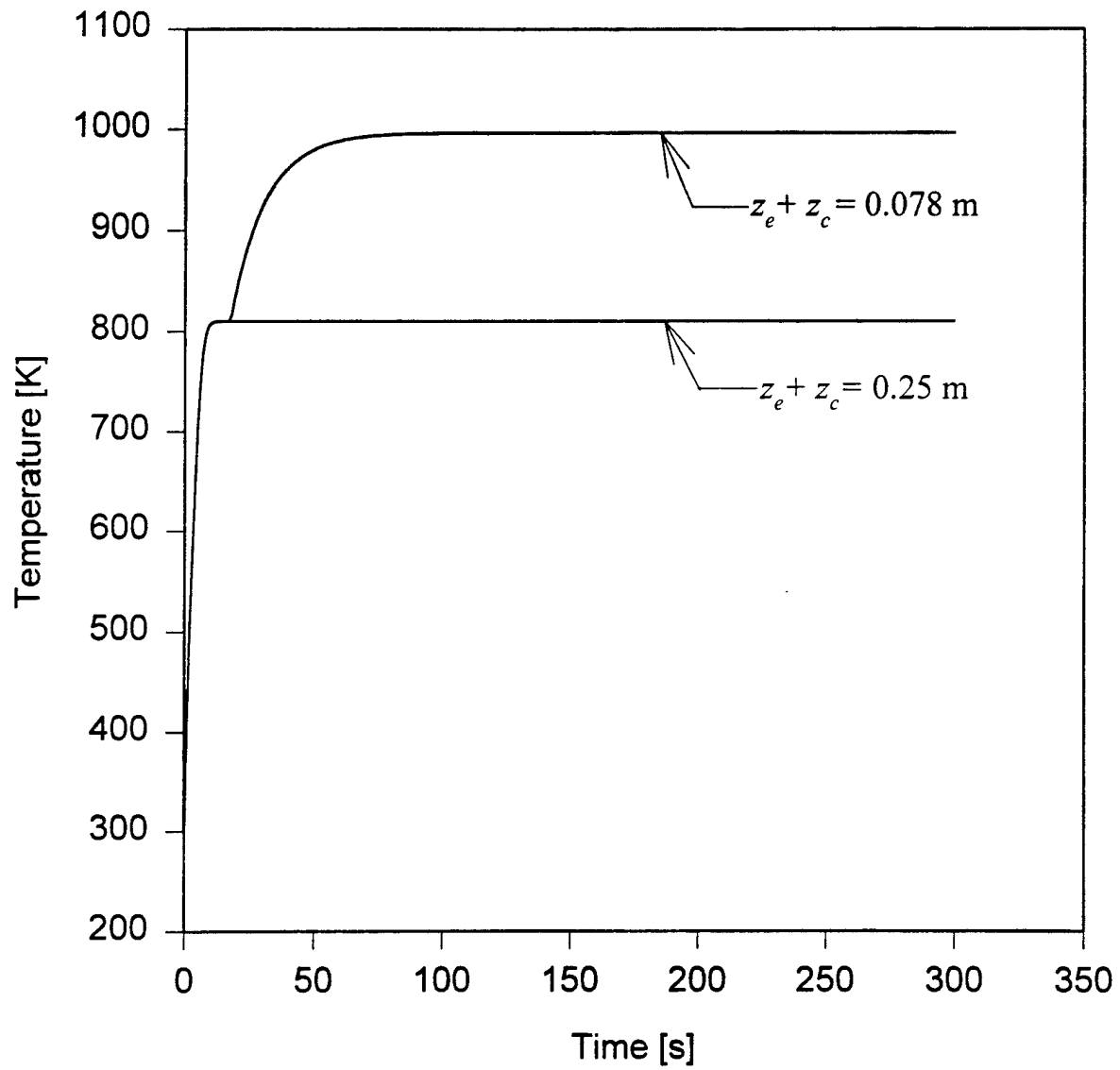


Fig. 8 Temperature response of the aft heat pipe.

Aft

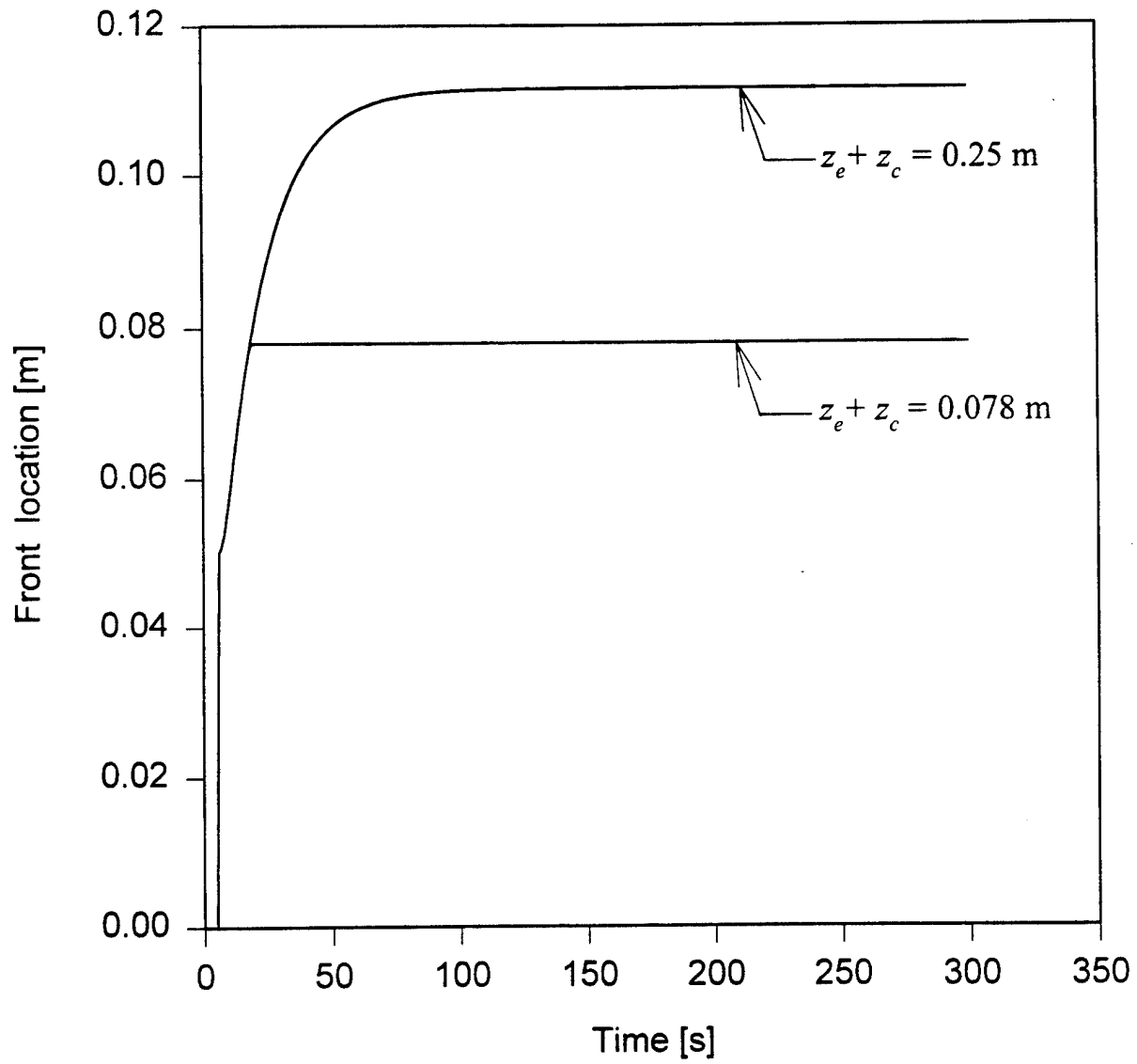


Fig. 9 Continuum front propagation of the aft heat pipe.

steady state is reached. Using the transient analysis, it has been found that the proper length of the condenser is critical for heat pipe design. If the condenser length is too short, the pipe temperature increases dramatically. Meanwhile, if it is too long, there is a risk of freezing the vaporized sodium in the inactive condenser region, causing dryout in the evaporator due to insufficient liquid.

Since the current transient model uses the lumped heat-capacity method, it cannot predict whether dryout occurs in the evaporator due to an insufficient amount of liquid to replenish the evaporator because of a suddenly applied heat load. Since a non-condensable gas helps the startup of the liquid-metal heat pipe from the frozen state, it is often desirable to include a little non-condensable gas in the vapor space. However, in the present case it is not possible to use non-condensable gas if the missile is severely maneuvering so that the orientation of the heat pipe is changing. The reason for this is as follows. When the evaporator is located below the condenser, the non-condensable gas must have a smaller molecular weight than that of the working fluid. Meanwhile, when the evaporator is above the condenser, the molecular weight of the non-condensable gas must be larger than that of the working fluid. Otherwise, the lighter gas will be swept to the evaporator and cover the wick surface causing a hot spot. The hot zone may then exceed the melting point of pipe material.

It is suggested that the wick structure for the fore heat pipe consist of interconnecting pores so as to spread the localized heat to the peripheral wick. For the aft heat pipe, however, the wick structure with interconnecting pores is not promising. This is because missile maneuvering may cause the melted liquid to collect in the trailing edge region. The most reliable wick structure may be axial grooves implanted with sintered metal fibers. The metal fibers must provide a sufficient wicking height for heat pipe operation against gravity. Each groove needs to be partially filled with metal fibers so that there is no cross communication with liquid. This is a non-standard wick design and involves some technical risk.

Both the steady-state analysis and the transient model rely on many assumptions. Also, the free-stream conditions cannot possibly be the same for each missile flight. Based on this, it is recommended that the heat pipe be made with a slightly extra length for the condenser than necessary so that some free molecular region is allowed. However, in order to confirm the feasibility of using the liquid-metal heat pipe to cool the hot region of the missile fin, experiments must be performed

under both transient and steady-state conditions. The heat pipe also needs to be tested at various tilt angles. The most critical tilt condition is that of the heat pipe in a vertical position with the evaporator above the condenser.

APPENDIX
LISTING OF THE COMPUTER PROGRAM

```

program HPWING
common/blk1/ao(8),a1(8),a2(8),a3(8),a4(8),a5(8)
common/blk2/airk,airrhov,aircp,airmuv,airgam,airPr,airR
common/blk3/subrhov,subrhol,subrhos,submuv,subhfg,subgam,
+   subhsl,subR,subcpl,subcps,subcpv,submul,subsig,subk
common/blk4/piperho,pipecp,wickrho,wickcp
common/blk5/Tprop
common/blk6/iwf
character*20 filechk,filedat,filein,filepot,fileout,junk
real Len,Me,Mc
real Tp(1500),z(1500)
C*****
C
C   VARIABLE NAME LIST
C
C   ao      =      coefficient in curve fit for working fluid
C   a1      =      coefficient in curve fit for working fluid
C   a2      =      coefficient in curve fit for working fluid
C   a3      =      coefficient in curve fit for working fluid
C   a4      =      coefficient in curve fit for working fluid
C   a5      =      coefficient in curve fit for working fluid
C
C   aircp   =      specific heat of air (J/kg K)
C   airgam  =      ratio of specific heats of air
C   airk    =      conductivity of air (W/m K)
C   airmuv  =      viscosity of air (N s/m^2)
C   airPr   =      Prandtl # of air
C   airR    =      gas constant of air (kJ/kg-K)
C   airrhov =      density of air (kg/m^3)
C   Ap      =      cross-sectional pipe area (m^2)
C   Av      =      calculated vapor core area by Simpson's rule (m^2)
C   Aw      =      cross-sectional wick area (m^2)
C   cval    =      effective volumetric heat capacity per unit length
C   cvalf   =      same as cval except for the free molecular region
C   delt    =      time increment (sec)
C   diam    =      equivalent vapor core diameter of heat pipe
C   diamlam =      vapor characteristic length used for Ttr calculation
C   epscp   =      accuracy-check value for cp
C   epsPr   =      accuracy-check value for Pr #
C
C   filechk =      checklist filename
C   filedat =      output property data for review
C   filein  =      design input data
C   filepot =      working fluid coefficient filename
C   fileout =      output filename
C
C   hbarc   =      avg heat transfer coefficient, cond
C   hbare   =      avg heat transfer coefficient, evap
C
C   istep   =      iteration step #
C
C   Len     =      length from stagnation point
C               =      to trailing edge along surface (m)
C   Mc      =      Mach # of flow over condenser
C   Me      =      Mach # of flow over evaporator
C   pi      =      3.14159
C   pipecp  =      specific heat of pipe (J/kg-K)
C   piperho =      density of pipe
C   por     =      porosity of wick
C

```

```

C      Qc      =      heat removal rate from condenser
C      Qe      =      heat load to evaporator
C      Qf      =      heat from continuum region to molecular flow region
C      Ql      =      latent heat (melting process)
C      Qs      =      sonic limit
C
C      re      =      recovery factor in evaporator section
C      rc      =      recovery factor in condenser section
C
C      subcpl   =      liquid cp of working substance
C      subcps   =      solid cp of working substance (J/kg-K)
C      subcpv   =      vapor cp of working substance (J/kg-K)
C      subgam   =      ratio of specific heats of working substance
C      subhfg   =      heat of vaporization of working substance
C      subk     =      conductivity of working substance
C      submul   =      liquid viscosity of working substance
C      submuv   =      vapor viscosity of working substance
C      subR     =      gas constant of working substance
C      subrhol  =      liquid density of working substance
C      subrhos  =      solid density of working substance
C      subrhov  =      vapor density of working substance
C      subsig   =      surface tension of working substance
C
C      Tf      =      temperature in free molecular region (K)
C      thkwall  =      thickness of wall (m)
C      thkwick  =      thickness of wick (m)
C
C      Tinfe   =      free stream temp over evaporator (K)
C      Tinfc   =      free stream temp over condenser (K)
C
C      tmax    =      max time to be considered (sec)
C      Tmelt   =      melt temp (K)
C      Tp      =      pipe temp (K)
C      Tprop   =      temp to evaluate properties at (K)
C      Trecc   =      recovery temp, condenser (K)
C      Trece   =      recovery temp, evaporator (K)
C      Trval   =      increment to Ttr to iteratively find Ttr
C      Tstagc  =      stagnation temp, condenser (K)
C      Tstage  =      stagnation temp, evaporator (K)
C      Tstarc  =      reference temp, condenser (K)
C      Tstare  =      reference temp, evaporator (K)
C      Ttr     =      transition temp (K)
C
C      wickcp   =      specific heat of wick (J/kg-K)
C      wickrho  =      density of wick
C
C      xo      =      location beyond which the flat plate
C                      correlation applies (m)
C
C      z       =      position along flat plate (m)
C      zc      =      length of condenser (m)
C      ze      =      length of flat plate (m)
C      zt      =      total available length of heat pipe (m)

```

```

C*****

```

```

write(*,*) '*****'
write(*,*) '*          *'
write(*,*) '*  Enter Working Fluid  *'
write(*,*) '*          *'

```

```

write(*,*) '* 1 = Sodium (Na)      *'
write(*,*) '* 2 = Potassium (K)   *'
write(*,*) '*                      *'
write(*,*) '*****'
write(*,*)
read(*,*) iwf
if(iwf.eq.1) filepot='sodium.dat'
if(iwf.eq.2) filepot='potassum.dat'
fileout='missile.out'
filechk='missile.chk'
filedat='missile.prp'
filein='missile.inp'
open(8,file=filepot,status='unknown')
open(9,file=filedat,status='unknown')
open(10,file=filechk,status='unknown')
open(11,file=fileout,status='unknown')
open(12,file=filein,status='unknown')

C*****

pi=2.*acos(0)

C   *** Time step in sec ***
C
write(*,*) 'Enter value for time increment : (>0.5)'
read(*,*) delt

C   *** Read in Liquid/Vapor Working Fluid Equation Coefficients ****

do 1 i=1,8
read(8,*) ao(i),a1(i),a2(i),a3(i),a4(i),a5(i)
1 continue

C   *** Design Input Variables ***
C
C   Data to be read in from file missile.inp
read(12,1000,end=2) junk
read(12,*) Len
read(12,1000,end=2) junk
read(12,*) ze
read(12,1000,end=2) junk
read(12,*) zt
read(12,1000,end=2) junk
read(12,*) diam
read(12,1000,end=2) junk
read(12,*) diamlam
read(12,1000,end=2) junk
read(12,*) thkwall
read(12,1000,end=2) junk
read(12,*) thkwick
read(12,1000,end=2) junk
read(12,*) por
read(12,1000,end=2) junk
read(12,*) Av
read(12,1000,end=2) junk
read(12,*) tmax
write(*,*) 'All input DATA has been read in.'
write(*,*)
write(*,*) 'Len      = ',Len
write(*,*) 'ze       = ',ze

```

```

write(*,*) 'zt      = ',zt
write(*,*) 'diam    = ',diam
write(*,*) 'diamlam= ',diamlam
write(*,*) 'thkwall= ',thkwall
write(*,*) 'thkwick= ',thkwick
write(*,*) 'por     = ',por
write(*,*) 'Av      = ',Av
write(*,*) 'tmax    = ',tmax
write(*,*)
write(11,*) 'Len     = ',Len
write(11,*) 'ze      = ',ze
write(11,*) 'zt      = ',zt
write(11,*) 'diam    = ',diam
write(11,*) 'diamlam= ',diamlam
write(11,*) 'thkwall= ',thkwall
write(11,*) 'thkwick= ',thkwick
write(11,*) 'por     = ',por
write(11,*) 'Av      = ',Av
write(11,*) 'tmax    = ',tmax
write(11,*)
goto 3

```

c Lengths are in meters

```

2      Len      = 0.12
       ze       = 0.05
       zt       = 0.25
       diam     = 0.0622
       diamlam  = 0.014
       thkwall  = 0.002
       thkwick  = 0.004
       por      = 0.7
       Av       = 0.00067
       tmax     = 20.

```

```

3      r1=diam/2.+thkwick+thkwall
       r2=diam/2.+thkwick
       r3=diam/2.

```

```

Ap=pi*r1**2. - pi*r2**2.
Aw=pi*r2**2. - pi*r3**2.

```

```

tmax=tmax*60.

```

c Working Substance

```

c      for sodium:
       if(iwf.eq.1) then
         Tmelt = 370.85
         subR  = 8315./23.
       endif

```

```

c      for potassium
       if(iwf.eq.2) then
         Tmelt = 336.4
         subR  = 8315./39.1

```

```

c      units of above are J/kg-K
       endif

```

c Flow Conditions

```

Tinfe = 1084.
Tinf = 299.8
Me = 0.8892
Mc = 0.75

airR = 287.
c units of above are J/kg-K
game = 1.4
gamc = 1.4

c Accuracy-Check Values

eps = 10.
epsPr = 0.01
epsTr = 5.00

c Set temp to Tinfe to evaluate properties for first iteration

c Velocity of flow (m/s)

uc = Mc * (gamc * airR * Tinf) ** 0.5
ue = Me * (game * airR * Tinfe) ** 0.5

c***** Begin Calculations *****
istep = 1
time = 0.
z(istep) = 0.
Tp(istep) = Tinf

c
c Want to consider Ttr to be a f(T); therefore, iterative
c Guess Ttrnew = 600. as a start point

Ttrnew = 600.
tprop = Ttrnew
call subprop
50 Ttr = 4990. * pi / subR * (submu / (subrho * diam * lam)) ** 2.
Trval = 1.0
if (abs(Ttr - Ttrnew) .lt. 100.) Trval = 0.01
if (abs(Ttr - Ttrnew) .lt. epsTr) goto 90
if (Ttr .lt. Ttrnew) then
Ttrnew = Ttrnew - Trval
tprop = Ttrnew
call subprop
goto 50
else
Ttrnew = Ttrnew + Trval
tprop = Ttrnew
call subprop
goto 50
endif

90 write(*,*) 'Ttransition = ', Ttr
write(11,*) 'Ttransition = ', Ttr
write(11,*)
write(11,*) 'Step t [s] Temp [K] Front [m] he [W/m^2-K]'
+hc [W/m^2-K]'
write(11,*) '-----'
+-----'

```

```

write(11,1030) istep,time,tp(istep),z(istep)

Tprop=Tinfe
call airprop

101   re=airPr**(1./3.)
      Tstage=Tinfe*(1.+((game-1.)/2.)*Me**2.)
      Trece=Tinfe+re*(Tstage-Tinfe)
      Tstare=(Tp(istep)+Tinfe)/2.+0.22*re*(game-1.)/2.*Me**2.*Tinfe
c
c   Now evaluate cp and Pr at Tstare; compare to assumed value.
c
      cpold=aircp
      Prold=airPr
      Tprop=Tstare
      call airprop
      cpnew=aircp
      Prnew=airPr

      diffcp=abs(cpnew-cpold)
      diffPr=abs(Prnew-Prold)
      if (diffcp.gt.epsdp .or. diffPr.gt.epsPr) goto 101

c   If OK, then evaluate hbar, else with new Pr go back and calc r
c   (actually go back to 101 and calculate based on properties at T*)

c       write(10,*) 'Pr# and cp converged to ',Prnew,cpnew
c       write(10,1010) istep,Tp(istep),Tstage,Trece,Tstare
c       write(10,*) 'airmuv, Len = ',airmuv,Len
c       write(10,*) 'airk, airrhov = ',airk,airrhov
c       write(10,*) 'ue, airPr = ',ue,airPr
      xo=pi*0.01*2./9.
      xl=xo/Len
      hbare=airk/Len*0.037*(airrhov*ue*Len/airmuv)**0.8*airPr**(1./3.)
+      *(1.-xl**0.8)/(1.-xl)
c       write(10,*) 'hbare = ',hbare

c -- Now do same process for condenser -----

      Tprop=Tinfc
      call airprop

107   rc=airPr**(1./3.)
      Tstagc=Tinfc*(1.+((gamc-1.)/2.)*Mc**2.)
      Trecc=Tinfc+rc*(Tstagc-Tinfc)
      Tstarc=(Tp(istep)+Tinfc)/2.+0.22*rc*(gamc-1.)/2.*Mc**2.*Tinfc
c
c   Now evaluate cp and Pr at Tstarc; compare to assumed value.
c
      cpold=aircp
      Prold=airPr
      Tprop=Tstarc
      call airprop
      cpnew=aircp
      Prnew=airPr

      diffcp=abs(cpnew-cpold)
      diffPr=abs(Prnew-Prold)
      if (diffcp.gt.epsdp .or. diffPr.gt.epsPr) goto 107

```

```

c      If OK, then evaluate hbar, else with new Pr go back and calc r
c      (actually go back to 107 and calculate based on properties at T*)

c      write(10,*) 'Pr# and cp converged to ',Prnew,cpnew
c      write(10,1011) istep,Tp(istep),Tstagg,Trecc,Tstarc

hbarc=airk/Len*0.037*(airrhov*uc*Len/airmuv)**0.8*airPr**(1./3.)
+      *(1.-xl**0.8)/(1.-xl)
c      write(10,*) 'hbarc = ',hbarc

Tprop=Tp(istep)
call subprop
call pipprop
Qs=subrhov*subhfg*Av*((subgam*subR*Tp(istep))/
+      (2.*(subgam+1.))**0.5)
Qe=2.*hbare*(Len-xo)*ze*(Trecc-Tp(istep))
Qc=2.*hbarc*(Len-xo)*(z(istep)-ze)*(Tp(istep)-Trecc)
if(Qc.lt.0.) Qc=0.

c      write(10,1020) Qs,Qe,Qc,subrhov,subhfg
      if(Tp(istep).gt.Ttr) then

+      cval=(piperho*pipecp*Ap) + (1.-por)*(wickrho*wickcp*Aw) +
+      por*(subrhol*subcpl*Aw)

      if(z(istep).ge.ze.and.z(istep).lt.(zt)) then
        Tp(istep+1)=Tp(istep) + (Qe-Qc-Qf)*delt/(cval*z(istep))
        Qf=Qs-Qc-(cval*(z(istep)-ze)*(Tp(istep+1)-Tp(istep))/delt)
        Quse=subrhol*por*Aw*subhsl
        Qf=Qf-Quse*(z(istep)-z(istep-1))
        Tprop=Tinf
        call subprop
        call pipprop
+      cvalinf=(piperho*pipecp*Ap) + (1.-por)*(wickrho*wickcp*Aw) +
+      por*(subrhos*subcps*Aw)
        Tprop=Tp(istep+1)
        z(istep+1)=z(istep) + Qf*delt/(cval*Tp(istep+1)-(cvalinf*
+      Tinf))

        elseif(z(istep).lt.ze) then
          z(istep+1)=ze
          Ql=subrhol*por*Aw*ze*subhsl
          if(imelt.gt.0) Ql=0.
          Tp(istep+1)=Tp(istep) + (Qe-Qc-Ql)*delt/(cval*ze)
c          write(10,*) '***** In the z lt ze spot',z(istep)

        elseif(z(istep).ge.(zt)) then
c          write(10,*) 'z is out of here -----'
          Tp(istep+1)=Tp(istep)+(Qe-Qc)*delt/(cval*(zt))
          z(istep+1)=zt
          imelt=0
          endif

        elseif(Tp(istep).lt.Tmelt) then
+      cval=(piperho*pipecp*Ap) + (1.-por)*(wickrho*wickcp*Aw) +
+      por*(subrhos*subcps*Aw)
          Tp(istep+1)=Tp(istep) + Qe*delt/(cval*ze)

c      write(10,*) ' In the Tp < Tmelt loop and cvalf= ',cvalf

```

```

elseif(Tp(istep).lt.Ttr.and.Tp(istep).gt.Tmelt) then
  cval=(piperho*pipecp*Ap) + (1.-por)*(wickrho*wickcp*Aw) +
+   por*(subrho1*subcpl*Aw)
  Tprop=Tp(istep)
  call subprop
  Q1=subrho1*por*Aw*ze*subhsl
  if(imeltm.eq.1) Q1=0.
  Tp(istep+1)=Tp(istep) + (Qe-Q1)*delt/(cval*ze)
  imelt=1
  imeltm=1
endif
istep=istep+1
tval=delt*(istep-1)
if(tval.gt.tmax) goto 999
write(11,1030) istep,tval,Tp(istep),z(istep),hbare,hbarc

  goto 101

999  continue
1000 format(a20)
1010 format('step = ',i4,' Tp = ',f8.3,' Toe= ',f8.3,' Tre= ',
+         f8.3,' T*r= ',f8.3)
1011 format('step = ',i4,' Tp = ',f8.3,' Toc= ',f8.3,' Trc= ',
+         f8.3,' T*c= ',f8.3)
1020 format('Qs = ',e10.3,' Qe = ',e10.3,' Qc = ',e10.3,' rho = ',
+         e7.2,' hfg = ',e7.2)
1030 format(1x,i4,f7.2,1x,f8.3,1x,e12.6,1x,e13.6,1x,e13.6)

  end

```

c***** Subroutine airprop *****

```

subroutine airprop
common/blk1/ao(8),a1(8),a2(8),a3(8),a4(8),a5(8)
common/blk2/airk,airrhov,aircp,airmuv,airgam,airPr,airR
common/blk3/subrhov,subrho1,subrhos,submuv,subhfg,subgam,
+   subhsl,subR,subcpl,subcps,subcpv,submul,subsig,subk
common/blk4/piperho,pipecp,wickrho,wickcp
common/blk5/Tprop

t=Tprop

c ----- Using curve fit data -----

airrhov = 2.45 - 5.72e-3*t + 5.32e-6*t**2. - 1.70e-9*t**3.
aircp   = 0.9422267 + 1.926976e-4*t
aircp   = aircp*1000.
airmuv  = 11.7858 + 0.6798*t - 3.8236e-4*t**2. + 1.1411e-7*t**3.
airmuv  = airmuv/1.e7
airk    = -6.40514e-3 + 1.35212e-4*t - 9.97069e-8*t**2. +
+       3.73997e-11*t**3.
airPr   = 0.838509 - 6.98285e-4*t + 9.82493e-7*t**2. -
+       3.96097e-10*t**3.
c      write(10,*) t,airrhov
end

```

c***** Subroutine pipprop *****

```

subroutine pipprop
common/blk1/ao(8),a1(8),a2(8),a3(8),a4(8),a5(8)
common/blk2/airk,airrhov,aircp,airmuv,airgam,airPr,airR
common/blk3/subrhov,subrhol,subrhos,submuv,subhfg,subgam,
+   subhsl,subR,subcpl,subcps,subcpv,submul,subsig,subk
common/blk4/piperho,pipecp,wickrho,wickcp
common/blk5/Tprop

t=Tprop

```

c ----- Using curve fit data -----

```

piperho = 8328.
pipecp  = 0.29418 + 6.51806e-4*t -4.99916e-7*t**2. +
+       1.63704e-10*t**3.
pipecp  = pipecp*1000.
c pipek  =
wickrho = piperho
wickcp  = pipecp
end

```

c***** Subroutine subprop *****

```

subroutine subprop
common/blk1/ao(8),a1(8),a2(8),a3(8),a4(8),a5(8)
common/blk2/airk,airrhov,aircp,airmuv,airgam,airPr,airR
common/blk3/subrhov,subrhol,subrhos,submuv,subhfg,subgam,
+   subhsl,subR,subcpl,subcps,subcpv,submul,subsig,subk
common/blk4/piperho,pipecp,wickrho,wickcp
common/blk5/Tprop
common/blk6/iwf

t=Tprop

```

c ----- Using B&K Handbook Least Square Data -----

```

subPlog=ao(1) + a1(1)*t + a2(1)*t**2. + a3(1)*t**3.
+          + a4(1)*t**4. + a5(1)*t**5.
Press=exp(subPlog)

subrhol=ao(2) + a1(2)*t + a2(2)*t**2. + a3(2)*t**3.
+          + a4(2)*t**4. + a5(2)*t**5.

c ** B&K gives nu, not mu .... (in the table of values)
submul=ao(3) + a1(3)*t + a2(3)*t**2. + a3(3)*t**3.
+          + a4(3)*t**4. + a5(3)*t**5.

subrhov=ao(4) + a1(4)*t + a2(4)*t**2. + a3(4)*t**3.
+          + a4(4)*t**4. + a5(4)*t**5.
subrhov=exp(subrhov)

c ** B&K gives nu, not mu .... (in the table of values)
submuv=ao(5) + a1(5)*t + a2(5)*t**2. + a3(5)*t**3.
+          + a4(5)*t**4. + a5(5)*t**5.

subsig=ao(6) + a1(6)*t + a2(6)*t**2. + a3(6)*t**3.
+          + a4(6)*t**4. + a5(6)*t**5.

```

```

      subhfg=ao(7) + a1(7)*t + a2(7)*t**2. + a3(7)*t**3.
+      + a4(7)*t**4. + a5(7)*t**5.

      subk=ao(8) + a1(8)*t + a2(8)*t**2. + a3(8)*t**3.
+      + a4(8)*t**4. + a5(8)*t**5.

      if(iwf.eq.1) then
c ----- Using curve fit data for Sodium -----
      subrhos=-0.22127*t + 1033.45338
      subcps = 0.5959051 + 4.838459e-3 *t - 1.450932e-5 *t**2.
+      + 1.73901e-8 *t**3.
      subcps = subcps*1000.
c----- Need to find actual data -----
      subhsl=113044.
c      units of above are J/kg
      subgam=1.67

c specific heat data from Incropera and DeWitt, Table A.7
      subcpl=1.3
      subcpl=subcpl*1000.

      write(9,1010) t,press,subrhol,submul,subrhov,submuv,subsig,
+subhfg,subk,subrhos,subcps,subgam,subcpl
      endif
      if(iwf.eq.2) then
c ----- Using curve fit data for Potassium -----

      subrhos=-0.16743*t + 914.46661
      subcps = 0.5073591 + 1.357728e-3 *t - 2.079707e-6 *t**2.
+      + 9.896415e-10 *t**3.
      subcps = subcps*1000.
c----- Need to find actual data -----
      subhsl=61127.28
c      units of above are J/kg
      subgam=1.4

c specific heat data from Incropera and DeWitt, Table A.7
      subcpl=0.75
      subcpl=subcpl*1000.

      write(9,1010) t,press,subrhol,submul,subrhov,submuv,subsig,
+subhfg,subk,subrhos,subcps,subgam,subcpl
      endif
1010 format(f8.3,10(1x,e9.2),1x,f3.1,1x,f7.2)

      end

```

REFERENCES

Brennan, P.J. and Kroliczek, E.J., "Heat Pipe Design Handbook," Volume II, NTIS, N81-70113, June 1979.

Chapman, A.J., Heat Transfer, 4th Edition, Macmillan Publishing Co., New York, 1984.

Chi, S.W., Heat Pipe Theory and Practice: A Sourcebook, Hemisphere Publishing Corp., Washington, 1976.

Eckert, E.R.G., "Survey of Boundary Layer Heat Transfer at High Velocities and High Temperatures," WADC Technical Report 59-624, Wright-Patterson Air Force Base, Ohio, April 1960.

Incropera, F.P. and DeWitt, D.P., Fundamentals of Heat Transfer, John Wiley and Sons, New York, 1981.

John, J.E.A., Gas Dynamics, 2nd Edition, Allyn and Bacon, Boston, 1984.

Kreith, F. and Bohn, M.S., Principles of Heat Transfer, 4th Edition, Harper & Row Publishers, New York, 1986.

Martinelli, R.C., Guibert, A.G., Morrin, E.H., and Boelter, L.M.K., "An Investigation of Aircraft Heaters VIII - A Simplified Method for the Calculation of the Unit Thermal Conductance over Wings," NACA ARR, March 1943.

Vargaftik, N.B., Tables on the Thermophysical Properties of Liquids and Gases, 2nd Edition, Hemisphere Publishing Corp., Washington, D.C., 1975.